Available online at www.sciencedirect.com
SCIENCE DIRECT®
Inorganica Chimica Acta 352 (2003) 238–246
Inorganica Chimica Acta
www.elsevier.com/locate/ica

# The synthesis, structural characterization, and in vitro anti-cancer activity of chloro(*p*-cymene) complexes of ruthenium(II) containing a disulfoxide ligand

Lynsey A. Huxham, Elizabeth L.S. Cheu, Brian O. Patrick, Brian R. James *

*Department of Chemistry, University of British Columbia, Vancouver, BC Canada V6T 1Z1*

Received 6 November 2002; accepted 9 January 2003

This paper is dedicated to Professor Martin Bennett, *the* connoisseur of Ru–arene chemistry, on the occasion of his retirement (65th birthday); one of us (B.R.J.) has known Martin for more than one half-life

**Abstract**

Two diruthenium(II) complexes $[RuCl_2(p\text{-cymene})]_2(\mu\text{-BESE})$ (**1**), $[RuCl_2(p\text{-cymene})]_2(\mu\text{-BESP})$ (**2**), and the mononuclear salt $[RuCl(p\text{-cymene})(BESE)]PF_6$ (**3**), containing the disulfoxides BESE and BESP, were synthesized and characterized by elemental analysis, and NMR and IR spectroscopies, and were shown to contain S-bound sulfoxide groups; the disulfoxides are $EtS(O)(CH_2)_nS(O)Et$, where $n = 2$ (BESE) or 3 (BESP). Complexes **1** and **3** were also characterized by X-ray crystallography. Preliminary in vitro tests of **1** and **3** were conducted using the MTT assay, which measures mitochondrial dehydrogenase activity as an indication of cell viability; these complexes showed in vitro anti-cancer activity against a human mammary cancer cell line (MDA-MB-435s) with $IC_{50}$ values of 360 and 55 μM, respectively.


*Keywords:* Crystal structures; Ruthenium complexes; *p*-Cymene complexes; Disulfoxide ligands; Anti-cancer activity

## 1. Introduction

The Pt-based drugs cisplatin and carboplatin are widely used anti-cancer agents [1], however, they are associated with high toxicity and some tumours resist these drugs. The exploration of Ru complexes for use as anti-cancer agents was initiated in attempts to find less toxic and more specific drugs [2]. An example of specificity is shown by the proposed behaviour of Ru(III) complexes, which suggests they may have low toxicity, as they bind transferrin, and therefore may target malignant cells as these up-regulate the expression of transferrin receptors on the cell membrane due to an increased iron requirement [2,3]. Some of the initial biological studies with Ru complexes involved *cis*- and *trans*-$RuCl_2(DMSO)_4$, and suggested these have anti-cancer properties and specifically anti-metastatic properties at high, yet relatively non-toxic, doses [4–7]. Complexes such as Na[*trans*-$RuCl_4(R_2SO)(L)$] and *mer*,*cis*-$RuCl_3(R_2SO)_2(L)$ ($L = NH_3$ or imidazole; $R_2SO$ = DMSO, and TMSO) have been synthesized as potential anti-cancer agents [8], and some initial work in this laboratory investigated $RuCl_2(R_2SO)_2$(nitroimidazole)$_2$ complexes and their potential as radiosensitizers [9,10]. The range of Ru(sulfoxide) complexes was then extended to include disulfoxide complexes, both to examine their in vitro activity [11] and to reduce the number of possible isomers formed during the preparation of $RuCl_2(R_2SO)_2$(nitroimidazole)$_2$ complexes. Thus, Yapp et al. characterized crystallographically disulfoxide complexes of the formula *cis*-$RuCl_2L_2$ [L = 1,2-bis(ethylsulfinyl)ethane (BESE), and 1,3-bis(methylsulfinyl)propane (BMSP)], and *trans*-$RuCl_2L_2$ [L = 1,2-bis(methylsulfinyl)ethane (BMSE), and 1,2-bis(propylsulfinyl)ethane (BPSE)], and preliminary in vitro experiments suggested that the *trans* complexes accumulate in cells and bind DNA to a

* Corresponding author. Tel.: +1-604-822 6645; fax: +1-604-822 2847.
*E-mail address:* brj@chem.ubc.ca (B.R. James).

0020-1693/03/$ - see front matter © 2003 Elsevier B.V. All rights reserved.
doi:10.1016/S0020-1693(03)00155-5

greater degree than the *cis* complexes [11]. Further studies by Cheu in this group have led to the characterization of *cis*-$RuCl_2L_2$ [L = 1,2-bis(butylsulfinyl)ethane (BBSE), 1,2-bis(pentylsulfinyl)ethane (BPeSE), 1,2-bis(cyclohexylsulfinyl)ethane (BCySE), and 1,3-bis(ethylsulfinyl)propane (BESP)], and *trans*-$RuCl_2L_2$ (L = BESE and BPSE) [12]. Diruthenium(II) complexes of the formula $[RuCl(L)H_2O]_2(\mu\text{-}Cl)_2$ (L = BESE, BPSE, and BBSE) and a mixed-valence species $[RuCl(BPSP)]_2(\mu\text{-}Cl)_3$ (BPSP = 1,3-bis(propylsulfinyl)propane), of which representative types have been structurally characterized, have been shown in vitro to have low toxicity and to bind DNA to a greater degree than mononuclear sulfoxide complexes [12]. The disulfoxides are of the general formula $RS(O)(CH_2)_nS(O)R$, where R is an alkyl group and $n = 2$ or 3.

Ruthenium(II) arene complexes have been shown to exhibit biological activity: complexes such as $[RuCl_2(C_6H_6)(metro)]$,[1] where metro = metronidazole (1-β-hydroxyethyl-2-methyl-5-nitroimidazole) [13], and $[RuCl_2(C_6H_6)(DMSO)]$ [14] have been studied for topoisomerase II activity and DNA damage ability, respectively, while reaction of $[RuCl_2(p\text{-cymene})]_2$ ($\mu\text{-}Cl_2$) with adenine (ade H) in the presence of $Ag(CF_3SO_3)$ forms $[Ru(adenine)(p\text{-cymene})]_4(CF_3SO_3)_4$ indicating the ability of Ru(*p*-cymene) complexes to interact with DNA bases [15]. Following such studies on Ru–arene systems, attempts in this laboratory to synthesize water-soluble disulfoxide complexes from the precursor $[RuCl(p\text{-cymene})]_2(\mu\text{-}Cl)_2$ led to the isolation of $[RuCl_2(p\text{-cymene})]_2(\mu\text{-BESE})$ (**1**), $[RuCl_2(p\text{-cymene})]_2(\mu\text{-BESP})$ (**2**) and $[RuCl(p\text{-cymene})(BESE)]PF_6$ (**3**), work which is described in this paper; **1** is the first structurally characterized, bridging disulfoxide Ru species. The preliminary in vitro anti-cancer activity of complexes **1** and **3** using the MTT assay [16] is also described (see Section 2.3).

During our studies, a report appeared by Dyson and coworkers on the structurally characterized $[RuCl_2(p\text{-cymene})(pta)]$ complex (pta = 1,3,5-triaza-7-phosphatricycol[3.3.1.1]decane) containing a Ru–P bond; the complex is water-soluble and exhibits pH-dependent DNA-binding [17]. Such half-sandwich Ru(II) arene complexes containing nitrogen ligands were also reported at about the same time by Sadler's group [18], who measured $IC_{50}$ values (concentration of drug required to reduce the cell culture growth by 50%) for a human ovarian cancer cell line with several of the complexes. Significantly, with respect to our paper, in vitro anti-cancer activity data for the $[RuCl(p\text{-cymene})(en)]PF_6$, an *N*,*N*′-analogue of our *S*,*S*′ complex **3**, were noted [18] (see Section 3.2).

[1] All the arene ligands mentioned in this paper are $\eta^6$-bonded, and the $\eta^6$ description is generally omitted for convenience.

## 2. Experimental

DMSO (Fisher), the dithioethers (Lancaster Synthesis), the deuterated solvents (Cambridge Isotopes), and all other solvents were used as supplied without further purification. $RuCl_3\cdot 3H_2O$ was donated by Johnson Matthey Ltd. and Colonial Metals Inc. The Et-$S(O)(CH_2)_nS(O)$Et disulfoxides BESE ($n = 2$) and BESP ($n = 3$) were synthesized by the acid-catalyzed, DMSO oxidation of the corresponding dithioethers (3,6-dithiaoctane and 3,7-dithianonane, respectively), following a literature procedure [19]; BESE (m.p. 148–149 °C) and BESP (m.p. 127–130 °C) were isolated in the *meso*-form from a mixture of diastereoisomers by three recrystallizations from EtOH, as we described earlier [11,12]. Of note, both *R*,*R*- and *S*,*S*-BESE have been isolated by methodology developed by Khiar's group [20], and are readily distinguished from the *meso*-form by $^1$H NMR [21]. $[RuCl(p\text{-cymene})]_2(\mu\text{-}Cl)_2$ was synthesized according to the procedure of Bennett et al. using $RuCl_3\cdot 3H_2O$ and α-phellandrene (Fluka) [22]. All syntheses were performed under $N_2$, unless otherwise stated, but all samples and products were stored at room temperature (r.t., ~20 °C) in air. Solution $^1$H NMR spectra ($D_2O$ or $CDCl_3$) were obtained using a Bruker AV-300 (300.13 MHz) FT-NMR spectrometer (s = singlet, bs = broad singlet, d = doublet, t = triplet, sp = septet, and m = multiplet; all coupling constants are given in Hz). $^1$H chemical shifts are given as $\delta$ (ppm), with reference to the residual solvent peak as the internal standard, relative to TMS. Infrared spectra (KBr, $cm^{-1}$) were obtained using an ATI Mattson Genesis Series FTIR instrument. Elemental analyses were obtained by Mr. P. Borda of this department, using a Carlo Erba Instruments EA 1108 CHN-O analyzer. Mass spectral analyses (LSIMS) were also obtained at the UBC facility. The X-ray crystallographic analyses are described in Section 2.2.

### 2.1. Syntheses

#### 2.1.1. $[RuCl_2(p\text{-cymene})]_2(\mu\text{-BESE})$ (**1**)

$[RuCl(p\text{-cymene})]_2(\mu\text{-}Cl)_2$ (200 mg, 0.32 mmol) and BESE (60 mg, 0.32 mmol) were placed under 1 atm $N_2$. $CH_2Cl_2$ (20 ml) was then added, via cannula, to the solids and the resultant deep red solution stirred for 30 min. The solvent was reduced in volume to 5 ml and hexanes (10 ml) were added to precipitate the red complex that was collected and dried in vacuo at 70 °C; yield 164 mg (64%). Attempts to increase the yield by refluxing or adding excess BESE were unsuccessful. Crystals suitable for X-ray crystallography were grown from slow evaporation of $CH_2Cl_2$ from a solution of the complex. *Anal*. Calc. for $C_{26}H_{42}Cl_4O_2S_2Ru_2$: C, 39.30; H, 5.33. Found: C, 39.46; H, 5.32%. IR $\nu_{so}$: 1082, 1110. Mass spectrum

[LSIMS, *m/z*, matrix: 3-nitrobenzylalcohol (3-NBA)]: 792 [$M^+$]. $^1$H NMR ($CDCl_3$, 300 MHz): $\delta$ 1.28 (d, *p*-cymene, $CH(CH_3)_2$, $J$ 6.90), 1.36 (t, BESE, $CH_3$, $J$ 7.50), 2.27 (s, *p*-cymene, $CH_3$), 2.82, 3.21 (bs, BESE, $CH_2S(O)CH_2$), 3.05 (sp, *p*-cymene, $CH(CH_3)_2$, $J$ 6.90), 5.55 (bs, *p*-cymene, $(CH_3)CHCH$), 5.63 (bs, *p*-cymene, $(CH_3)C(CHCH)$. There are also peaks corresponding to $[RuCl(p\text{-cymene})]_2(\mu\text{-}Cl)_2$, formed via dissociation of **1** (see Section 3.1) at $\delta$ 1.26 (d, *p*-cymene, $CH(C(CH_3)_2$, $J$ 6.92), 2.14 (s, *p*-cymene, $CH_3$), 2.90 (sp, *p*-cymene, $CH(CH_3)_2$, $J$ 6.92), 5.31 (d, *p*-cymene, $(CH_3)C(CHCH$, $J$ 5.94), 5.44 (d, *p*-cymene, $(CH_3)C(CHCH$, $J$ 5.94).

### 2.1.2. [$RuCl_2$(*p*-cymene)]$_2$($\mu$-BESP) (**2**)

The procedure used for synthesizing **2** is that given for **1** but using $[RuCl(p\text{-cymene})]_2(\mu\text{-}Cl)_2$ (50 mg, 0.081 mmol) and BESP (15 mg, 0.081 mmol). The volume of the solvent was reduced to 2 ml and $Et_2O$ (10 ml) was used to precipitate the red complex that was washed twice with $Et_2O$, collected, and dried in vacuo at 70 °C; yield 20 mg (30%). *Anal*. Calc. for $C_{27}H_{44}Cl_4O_2S_2Ru_2$: C, 40.11; H, 5.48. Found: C, 39.92; H, 5.57%. IR $\nu_{so}$: 1074, 1082, 1090, 1095, 1108, 1116, 1122. Mass spectrum [LSIMS, *m/z*, matrix: thioglycerol]: 809 [$M^+$]. $^1$H NMR ($CDCl_3$, 300 MHz): $\delta$ 1.29 (d, *p*-cymene, $CH(CH_3)_2$, $J$ 6.89), 1.34 (t, BESP, $CH_3$, $J$ 7.50), 2.28 (s, *p*-cymene, $CH_3$), 2.35 (m, BESP, $CH_2CH_3$), 2.80 (bs, BESP, $CH_2CH_2CH_2$), 3.05 (m, BESP, $CH_2CH_2CH_2$), 3.08 (sp, *p*-cymene, $CH(CH_3)_2$, $J$ 6.89), 5.55 (bs, *p*-cymene, $(CH_3)C(CHCH)$, 5.63 (bs, *p*-cymene, $(CH_3)C(CH$–CH). Again, because of dissociation of **2**, peaks due to $[RuCl(p\text{-cymene})]_2(\mu\text{-}Cl)_2$ are seen.

### 2.1.3. [$RuCl$(*p*-cymene)(*BESE*)]$PF_6$ (**3**)

*2.1.3.1. Method 1.* $[RuCl(p\text{-cymene})]_2(\mu\text{-}Cl)_2$ (50 mg, 0.081 mmol) and BESE (30 mg, 0.16 mmol) were dissolved overnight in stirred $H_2O$ (20 ml) under 1 atm $N_2$ or air to give a yellow solution. $NH_4PF_6$ (26 mg, 0.16 mmol) was then added and the solution volume reduced to 5 ml. The mixture was then filtered through Celite to remove traces of Ru metal, and the filtrate left overnight, when yellow crystalline material formed. This was filtered off and dried in vacuo at 70 °C; yield 30 mg (31%). The yield was improved to 62 mg (62%) by reducing the solvent volume to 1 ml and adding MeOH (3 ml). X-ray quality needle crystals were grown from the complex dissolved in a 1:1 mixture of $H_2O$ and MeOH. *Anal*. Calc. for $C_{16}H_{28}ClO_2S_2RuPF_6$: C, 32.14; H, 4.72. Found: C, 32.24; H, 4.77%. IR $\nu_{so}$: 1072, 1090, 1107, 1119, 1132, 1142. $\Lambda_M$ ($H_2O$): 75 $\Omega^{-1}$ cm$^2$ mol$^{-1}$. $^1$H NMR ($D_2O$, 300 MHz): $\delta$ 1.06 (d, 6H, *p*-cymene $CH(CH_3)_2$, $J$ 6.93), 1.40 (t, 6H, BESE $CH_3$), 2.06 (s, 3H, *p*-cymene, $CH_3$), 2.70 (sp, H, *p*-cymene, $CH(CH_3)_2$), 3.40–3.70 (m, 8H, BESE $CH_2S(O)$–$CH_2CH_3$), 6.28 (s, 4H, *p*-cymene, $CHCH$). $^1$H NMR ($CDCl_3$, 300 MHz): $\delta$ 1.24 (d, 6H, *p*-cymene $CH(CH_3)_2$, $J$ 6.93), 1.55 (t, 6H, BESE $CH_3$), 2.25 (s, 3H, *p*-cymene $CH_3$), 2.95 (sp, H, *p*-cymene, $CH(CH_3)_2$), 3.45 (m), 3.75 (m), 3.52 (s) (8H, BESE, $CH_2S(O)CH_2CH_3$), 6.12 (s, 4H, *p*-cymene, $CHCH$).

*2.1.3.2. Method 2.* Complex **1** (50 mg, 0.063 mmol) was completely dissolved in $H_2O$ (10 ml) and $NH_4PF_6$ (21 mg, 0.13 mmol) was added. The solution was concentrated to 5 ml, filtered and left overnight, when yellow crystals formed. The $^1$H NMR data agree with those reported in method 1.

## 2.2. X-ray crystallographic analyses of *1* and *3*

The structures of both **1** and **3** were solved by direct methods and expanded using Fourier techniques; the H-atoms were included at calculated positions, but not refined. Selected crystallographic data appear in Table 1. An orange red, block crystal of **1** ($\sim 0.30 \times 0.20 \times 0.10$ mm$^3$) and a yellow prism crystal of **3** ($\sim 0.10 \times 0.10 \times 0.10$ mm$^3$) were each mounted on a glass fibre. All measurements were made on a Rigaku/ADSC CCD area detector with graphite mono-chromated Mo K$\alpha$ radiation ($\lambda = 0.71069$ Å). The cell constants for **1**, based on 10 069 reflections with $2\theta = 3.6$–$58.3°$, corresponded to a primitive triclinic cell with space group $P\bar{1}$

Table 1
Selected crystallographic data[a] for $[RuCl_2(p\text{-cymene})]_2(\mu\text{-BESE})$ (**1**) and $[RuCl(p\text{-cymene})(BESE)]PF_6$ (**3**)

| | **1** | **3** |
|---|---|---|
| Empirical formula | $C_{26}H_{42}O_2S_2Cl_4Ru_2$ | $C_{16}H_{28}O_2F_6PS_2ClRu$ |
| Formula weight | 794.69 | 598.00 |
| Crystal system | triclinic | orthorhombic |
| Space group | $P\bar{1}$ (no. 2) | *Pbca* (no. 61) |
| Unit cell dimensions | | |
| $a$ (Å) | 9.7899(4) | 16.9476(6) |
| $b$ (Å) | 12.4235(9) | 15.1712(4) |
| $c$ (Å) | 14.431(1) | 35.756(2) |
| $\alpha$ (°) | 75.226(3) | |
| $\beta$ (°) | 72.818(2) | |
| $\gamma$ (°) | 68.101(3) | |
| $V$ (Å$^3$) | 1534.9(2) | 9193(1) |
| $Z$ | 2 | 16 |
| $\rho_{calc}$ (g cm$^{-3}$) | 1.72 | 1.73 |
| $\lambda$ (Å) | 0.71069 | 0.71069 |
| $\mu$ (cm$^{-1}$) | 14.91 | 11.08 |
| Observations $I > 0.00\sigma(I)$ | 6266 | 10211 |
| Variables | 325 | 575 |
| Observations $I > 3\sigma(I)$ | 5557 | 5195 |
| Final $R$ indices [$I > 3\sigma(I)$] | $R = 0.029$, $R_w = 0.053$ | $R = 0.028$, $R_w = 0.032$ |
| $R$ indices (all data) | $R = 0.042$, $R_w = 0.095$ | $R = 0.064$, $R_w = 0.082$ |
| Goodness-of-fit | 1.56 | 0.68 |

[a] $R = \Sigma||F_o| - |F_c||/\Sigma|F_o|$, $R_w = (\Sigma\, w(\Sigma|F_o| - |F_c|^2/(\Sigma\, w/|F_o|^2)^{1/2}$.

(no. 2). The data were collected at $-100 \pm 1$ °C to a maximum $2\theta$ value of 58.3° and were collected in 0.50° oscillations with 35.0 s exposures. A sweep of data was done using $\phi$ oscillations from 0.0 to 190.0° at $\chi = -90.0°$ and a second sweep was performed using ω oscillations between $-18.0$ and 23.0° at $\chi = -90.0°$. The crystal to detector distance was 39.17 mm and the detector swing angle was $-5.50°$. Of the 13880 reflections that were collected, 6270 were unique ($R_{int} = 0.030$); equivalent reflections were merged. Data were collected and processed using the d*TREK program [23]. The linear absorption coefficient, $\mu$, for Mo Kα radiation was 14.9 $cm^{-1}$, and the data were corrected for Lorentz and polarization effects.

For complex **3**, cell constants based on 24 488 reflections with $2\theta = 5.0–55.9°$ corresponded to a primitive orthorhombic cell with space group *Pbca* (no. 61). The data were collected as above in 0.30° oscillations with 28.0 s exposures. A sweep of data was done using ϕ oscillations from 0.0 to 189.9° at $\chi = -90.0°$ and a second sweep was performed using ω oscillations between $-17.0$ and 22.9° at $\chi = -90.0°$. The crystal to detector distance was 38.12 mm and the detector swing angle was $-5.56°$. The data reduction was generally as described above with some differences: of the 63 971 reflections collected, 10 959 were unique ($R_{int} = 0.092$); $\mu$ was 11.1 $cm^{-1}$.

Complex **1** crystallizes with two half-molecules in the asymmetric unit (i.e. each half-molecule resides on an inversion centre). The full-matrix least-squares refinement, based on 5557 observed reflections ($I > 3\sigma(I)$) and 325 variable parameters, converged with unweighted ($R$) and weighted ($R_w$) agreement factors of 0.029 and 0.053, respectively.

Complex **3** crystallizes with two 1:1 salt moieties (each is a different conformation) in the asymmetric unit. Refinement, based on 5195 observed reflections ($I > 3\sigma(I)$) and 575 variable parameters, converged with agreement factors of 0.028 ($R$) and 0.032 ($R_w$).

### 2.3. Biological MTT assay

3-(4,5-Dimethylthiazol-2-yl)-2,5-diphenyltetrazolium bromide (MTT) was purchased from Sigma. All media and solutions were purchased sterile, or were sterilized through 0.2 μm filters (150 ml flask: 33 mm neck, Corning) and kept under sterile conditions before use.

A need to determine the sensitivity of specific tumors and individualize therapy has led to the development of a number of in vitro assays, one of which is the MTT assay that measures mitochondrial dehydrogenase activity as a reflection of cell viability; this shows considerable promise in the screening and evaluation of potential new anti-cancer agents [16,24,25]. The yellow tetrazolium form of MTT is reduced, in active cells, by mitochondrial dehydrogenases to form purple formazan crystals [16]. A colourimetric, optical density (OD) determination then quantifies the percentage of viable cells (i.e. metabolically active after incubation with the test complex). The growth inhibitory effect of the added complex is expressed as a percentage of the control processed at the same time [(OD of treated sample/OD of control) × 100]. The percentages are then graphed for each concentration tested in order to create a dosage effect curve, and the curves are analyzed for the $IC_{50}$ value.

The cells used were obtained from a human mammary cell line MDA-MB-435s. The cells were routinely maintained with Dulbecco's Modified Eagle's medium (Stem Cell Technologies) supplemented with 10% fetal bovine serum, at 37 °C in a NAPCO water-jacketed, $CO_2$-incubator under an atmosphere of 95% air/5% $CO_2$. The cells were trypsinized biweekly with 0.25% trypsin–EDTA (2 ml, Gibco) at 37 °C for 3–4 min and $1 \times 10^5$ cells were plated in a T-25 flask containing α+/+ medium ( ~ 5 ml). For experiments, $1 \times 10^6$ cells were plated in a T-75 flask with α+/+ medium (20 ml) and grown for several doubling times, changing the medium every few days.

For each complex tested, a 96-well plate was prepared by adding $1 \times 10^4$ cells in 100 μl of medium to each experimental and control well. Medium (200 μl) was then added to one column of wells to serve as a blank. The outside wells of the plate were filled with sterile $H_2O$ (200 μl), and the plate was incubated for 24 h at 37 °C under the air/$CO_2$ mixture. At the 23rd hour, the Ru complex was dissolved in phosphate buffer saline solution (PBS) (4 °C), and the solution vortexed and left for 1 h before filtering through a 0.2 μm needle filter (Nalgen). The stock solution of the complex was then serially diluted with α+/+ medium in six-well plates (Falcon), according to prepared concentrations, and then added to the experimental wells, starting with the lowest concentration and ending with the highest concentration. Medium (100 μl) was then added to the control wells and the plate was incubated for 68 h, when the MTT (50 μl of 2.5 mg $ml^{-1}$) was added and the plate incubated for a further 4 h. The wells were then aspirated to remove all liquid, and DMSO (150 μl) was added to each well to dissolve the formazan crystals. The plates were vortexed, and the proportion of formazan was quantified by absorbance readings at 570 nm using a Molecular Devices SPECTRAmax PLUS plate reader.

## 3. Results and discussion

### 3.1. Characterization and chemistry of complexes 1–3

The ORTEP diagram for **1** (Fig. 1) shows two typical piano-stool type moieties joined by the bridged S-bound

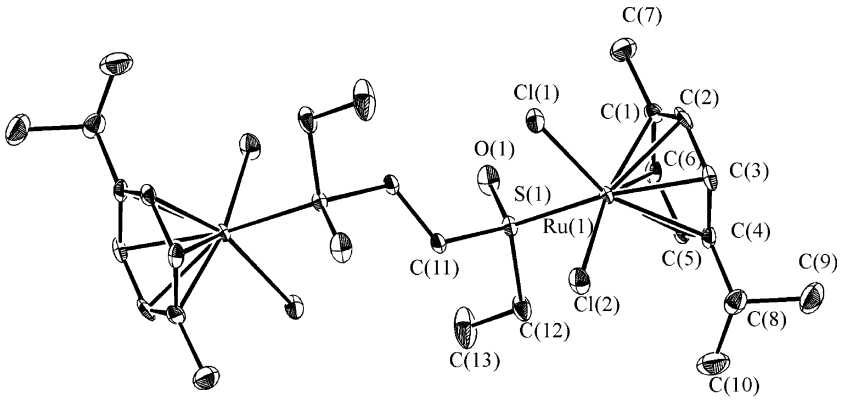


Fig. 1. A molecular structure representation (ORTEP) of one of the crystallographically independent half-molecules of $[RuCl_2(p\text{-cymene})]_2$(μ-BESE) (**1**), with 50% probability thermal ellipsoids shown; H-atoms are omitted for clarity.

disulfoxide *meso*-BESE; the two sulfur-atoms within each molecule of the centrosymmetric structure have opposite chiralities, consistent with synthesis using *meso*-BESE. The $\eta^6$-*p*-cymene ligands (one at each Ru) are *syn*, with the $^i$Pr groups pointing in different directions. Selected bond lengths and bond angles of **1** and **3** are given in Table 2. The geometries of the coordinated sulfoxide and *p*-cymene moieties are typical of those well established in Ru(II)–sulfoxide [11,26] and Ru(II)–*p*-cymene complexes [17], and the Ru–Cl distances are normal [17,27]. The S–O bond lengths for **1** are similar, for example, to those for the S-bound sulfoxides in *cis*-$RuCl_2$(BESE)$_2$ [11].The Ru–S bond lengths for **1** are just shorter than the sum of the covalent radii of Ru and S (2.37 Å) [28], suggesting little π-back-donation between the Ru- and S-atoms. The Ru–S bond lengths for complex **1** are significantly longer than the range of values Ru–S (2.271–2.308(8) Å) seen for *cis*-$RuCl_2$(BESE)$_2$ [11], perhaps indicating a general '*trans*' influence of the organometallic ligand greater than that of Cl- or S-bound sulfoxide. The sulfoxide moieties in **1** have the usual distorted trigonal pyramid geometry with C–S–C angles of 100.2 and 102.5°, and C–S–O angles of 103.9–108.4° [26]; these values are close to the average of 100.3(1)° (mean of 310 values) and 107.34(7)° (mean of 648 values), respectively, found in metal S-bonded sulfoxide complexes [26]. The $RuCl_2$(*p*-cymene) components are essentially identical to that of $RuCl_2$(*p*-cymene)(pta) mentioned in Section 1 [17]. The IR bands at 1082 and 1110 $cm^{-1}$ are assigned to $\nu_{SO}$ of the S-bound sulfoxide [11]. The $^1$H NMR spectrum of **1** in $CDCl_3$ at room temperature shows peaks that correspond to those of $[RuCl(p\text{-cymene})]_2(\mu\text{-Cl})_2$ (see Section 2.1.1), implying the presence of an equilibrium (see Eq. (1) and Fig. 4). There are also downfield shifted signals, corresponding to the coordinated *p*-cymene protons of **1**: the singlet at $\delta$ 2.27 is due to the $CH_3$ group (**A**) (Fig. 2); the aromatic protons (**B** and **C**), seen as broad singlets at $\delta$ 5.63 and

Table 2
Selected bond lengths (Å) and bond angles (°) for $[RuCl_2(p\text{-cymene})]_2$(μ-BESE) (**1**) and $[RuCl(p\text{-cymene})(BESE)]PF_6$(**3**)

| | **1** [a] | **3** [b] |
|---|---|---|
| *Bond lengths* | | |
| S–O | 1.476(2) | 1.461(3) |
| | 1.483(2) | 1.467(3) |
| S–C | 1.810(3) | 1.791(4) |
| | 1.829(3) | 1.796(4) |
| | 1.801(3) | 1.798(4) |
| | 1.828(3) | 1.807(4) |
| $Ru–C_{average}$ | 2.203 | 2.247 |
| | 2.209 | |
| Ru–Cl | 2.402(7) | 2.385(1) |
| | 2.407(7) | |
| | 2.394(8) | |
| | 2.414(7) | |
| Ru–S | 2.335(7) | 2.288(1) |
| | 2.345(7) | 2.302(1) |
| *Bond angles* | | |
| C–S–O | 108.2(2) | 108.2(2) |
| | 108.4(1) | 109.1(2) |
| | 103.9(1) | 107.0(2) |
| | 107.1(1) | 107.0(2) |
| C–S–C | 100.2(1) | 101.0(2) |
| | 102.5(1) | 103.3(2) |
| Cl–Ru–S | 85.70(2) | 87.37(4) |
| | 86.89(3) | 89.40(4) |
| | 86.13(2) | |
| | 86.23(3) | |
| Ru–S–O | 114.15(9) | 115.3(1) |
| | 115.4(1) | 118.1(1) |
| S–Ru–S | | 83.73 |
| Cl–Ru–Cl | 88.39(3) | |
| | 90.47(3) | |

[a] The two values arise because of two half-molecules in the asymmetric unit (Section 2.2).

[b] Data are taken from the structural conformer shown in Fig. 3(a).

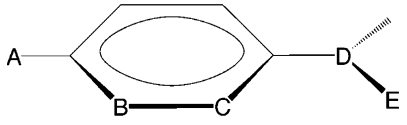


Fig. 2. The structure of *p*-cymene showing labelling of the protons.

5.55, respectively, are assigned based on those reported by Bennett et al. [22]; the septet at $\delta$ 3.05 and the doublet at $\delta$ 1.28 correspond to the CH proton (**D**) and the $CH_3$ protons (**E**), respectively, of the $^{i}$Pr group. The triplet at $\delta$ 1.36 results from the $CH_3$ groups of BESE, both coordinated and free. The broad peaks at $\delta$ 2.82 (bs), and 3.21 (bs) correspond to the $CH_2$ protons of bridged and free BESE.

At room temperature, **1** at $10^{-3}$ M in $CDCl_3$ dissociates to $\sim$60%; at 243 K, the degree of dissociation is $\sim$35%, as estimated by changes in the intensities of the $\delta$ 2.27 and 2.14 signals for **1** and [RuCl(*p*-cymene)]$_2$(μ-Cl)$_2$, respectively. *K* for equilibrium (1) at $\sim$20 °C is thus $\sim 9 \times 10^{-4}$ M. Additions of BESE to $CDCl_3$ solutions of **1** give increasing amounts of **1**, formed in good agreement with such a *K* value.

$$[RuCl_2(p\text{-cymene})]_2(\mu\text{-BESE})\ (\mathbf{1}) \overset{K}{\rightleftharpoons} [RuCl(p\text{-cymene})]_2 \times (\mu\text{-Cl})_2 + \text{BESE} \quad (1)$$

[RuCl$_2$(*p*-cymene)]$_2$(μ-BESP) (**2**) was prepared by the method used to synthesize **1**, and the structure is assumed to be analogous to that of **1**. The $^1$H NMR signals for **2** are at $\delta$ 1.29 (d), 1.34 (t), 2.28 (s), 2.80 (bs), 2.35 (m), 3.05 (m), 3.08 (sp), 5.55 (bs), and 5.63 (bs) and, except for the 'extra' peak at $\delta$ 2.35 (which results from the 'extra' $CH_2$ group on the BESP backbone), can be assigned as for **1**. The $^1$H NMR also shows peaks due to the *p*-cymene precursor and some free BESP, again giving evidence for a dissociative equilibrium analogous to that shown in Eq. (1). Seven IR bands appear in the $\nu_{SO}$ (S-bonded) region suggesting more than one conformer in the solid state (see below for **3**). Several other homo-bimetallic complexes containing a bridging disulfoxide are known, examples including those of Cu(II) [29], Sn(IV) [30] and Pt(II) [31], but those with an *S*,*S*′-bound disulfoxide are rare; an example is [PtCl$_2$(PEt$_3$)]$_2$(μ-PhS(O)(CH$_2$)$_2$S(O)Ph) [31] but, to our knowledge, **1** and **2** are the first Ru bridged-disulfoxide complexes. There are $Ru_2^{II}$ complexes containing (μ-*S*,*O*–R$_2$SO), with both S- and O-binding from a monosulfoxide [32].

The yellow [RuCl(*p*-cymene)(BESE)]PF$_6$ (**3**) was synthesized from [RuCl(*p*-cymene)]$_2$(μ-Cl)$_2$, BESE and $NH_4PF_6$ in water, or by dissolving **1** in water and adding $NH_4PF_6$; the complex was isolated by crystallization from concentrated aqueous solutions or by precipitation on addition of MeOH. The relatively low yield via crystallization results from high solubility of the complex in $H_2O$, and also in method 1 some Ru metal is seen. The conductivity data correspond to the presence of a 1:1 electrolyte [33]. The ORTEP structures of the two conformers of the cation found in the asymmetric unit are shown in Fig. 3 (the $PF_6^-$ counterion is omitted). The structure in Fig. 3(a) shows a non-bridging, $\eta^2$-*S*,*S*′-bound *meso*-BESE, whose S=O moieties are *syn* (and the chloro ligand *anti*) to the *p*-$CH_3$ group of the $\eta^6$-*p*-cymene; the other conformer (Fig. 3(b)) shows the *meso*-BESE, but now the S=O groups are *syn* (and the chloro ligand *anti*) to the $^{i}$Pr group of the cymene. The bond lengths and angles of both conformers are very similar, and only those for the conformer shown in Fig. 3(a) are given in Table 2. The S–O bond lengths are essentially the same as in **1**, while the somewhat shorter Ru–S bond lengths might result from: (a) the S-atoms not being trans to the centroid of the *p*-cymene ring (see above); or (b) a higher degree of π-back-bonding between the Ru- and S-atoms than in **1** [26,28]. The C–S–C and C–S–O angles are very much as in **1**. The

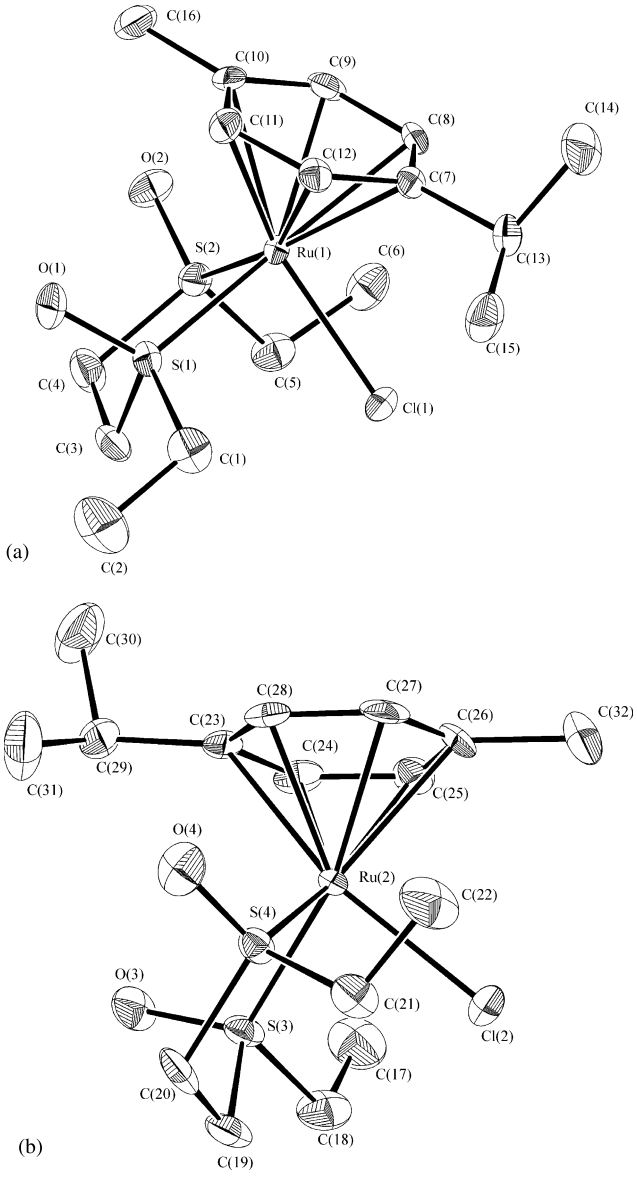


Fig. 3. ORTEP molecular structures of the two conformers of [RuCl(*p*-cymene)(BESE)]$^+$ (**3**) with 50% probability thermal ellipsoids shown, H-atoms being omitted for clarity; the enantiomorph shown in (a) has *R*-chirality at S(1) and *S*-chirality at S(2), while the enantiomorph shown in (b) has *S*-chirality at S(3) and *R*-chirality at S(4).

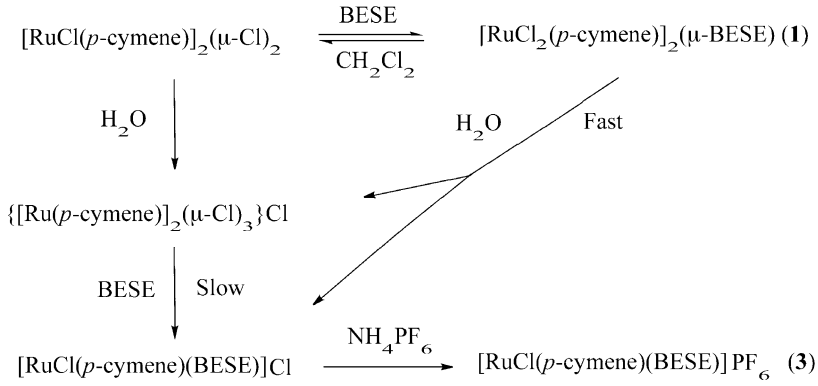


Fig. 4. The proposed solution behaviour of $[RuCl_2(p\text{-cymene})]_2(\mu\text{-BESE})$ (**1**), and the subsequent formation of $[RuCl(p\text{-cymene})(BESE)]PF_6$ (**3**).

bite angle (83.73°) of the BESE at the Ru in **3** is somewhat smaller than those seen (87.69 and 87.19°) in *cis*-$RuCl_2(BESE)_2$ [11]. The Cl–Ru–S angles in **3** are about 2–3° greater than in **1**, while those in $RuCl_2(BESE)_2$ are generally greater still (in the 89.36–91.83° range) [11].

The $^1H$ NMR spectrum of **3** in $D_2O$ shows just one triplet at $\delta$ 1.40 for the $CH_3$ groups of the BESE revealing that they are equivalent and that the molecule is fluxional in solution with presumed rotation of the *p*-cymene ligand. The eight $CH_2$ protons of the BESE ligand appear as a broad multiplet between $\delta$ 3.40–3.70. The singlet at $\delta$ 2.06 corresponds to the coordinated *p*-cymene protons **A**, and the doublet at $\delta$ 1.06 and septet at $\delta$ 2.70 correspond to the isopropyl protons **E** and **D**, respectively. Unlike in **1** and **2**, the aromatic protons **B** and **C** appear as a singlet ($\delta$ 6.28). A singlet was also reported for the corresponding protons of the *p*-cymene complexes $RuX_2(p\text{-cymene})L$, where X is a halogen and L is a tertiary phosphine or arsine [22]; no rationale was offered, and we can offer nothing more constructive than possible accidental degeneracy. The $\nu_{SO}$ IR data are again consistent with S-bound disulfoxide, with the multitude of bands presumably resulting from the presence of two conformers and solid state effects.

The precursor for **1** and **2**, $[RuCl(p\text{-cymene})]_2(\mu\text{-Cl})_2$, dissolves in water and is believed to form the cationic complex $\{[Ru(p\text{-cymene})]_2(\mu\text{-Cl})_3\}Cl$, as suggested by Bennett et al. [22]. The $^1H$ NMR spectrum for this species in $D_2O$ shows a singlet at $\delta$ 2.06 for the **A** protons, doublets at $\delta$ 5.48 and 5.70 for the aromatic protons **C** and **B**, respectively, and a doublet at $\delta$ 1.19 and septet at $\delta$ 2.73 for the **E** and **D** protons, respectively. There are also small signals shifted slightly downfield from each of those noted above, and these may be due to a species such as $[RuCl(p\text{-cymene})(D_2O)_2]^+$ [22,34].

When **1** is dissolved in $D_2O$, the $^1H$ NMR spectrum shows signals at $\delta$ 1.07 (d), 1.40 (t), 2.06 (s), 2.71 (sp), 3.40–3.65 (m), and 6.29 (s), which correspond to those of the cation of the characterized $[RuCl(p\text{-cymene})(BESE)]PF_6$ (**3**), and small signals at $\delta$ 1.17 (t), 2.84 (m), and 3.13 (m), which are those for free BESE; small peaks are seen also for $\{[Ru(p\text{-cymene})]_2(\mu\text{-Cl})_3\}Cl$ but these disappear over ~24 h. If $[RuCl(p\text{-cymene})]_2(\mu\text{-Cl})_2$ is placed in $D_2O$ and 2 equiv. of BESE are added, the $^1H$ NMR spectrum shows peaks for free BESE and these disappear over ~24 h with complete generation of $[RuCl(p\text{-cymene})(BESE)]Cl$. The $^1H$ NMR data imply that in water **1** dissociates rapidly to give mainly $[RuCl(p\text{-cymene})(BESE)]Cl$ and some $\{[Ru(p\text{-cymene})]_2(\mu\text{-Cl})_3\}Cl$, while the latter species reacts slowly with BESE to generate the former species. The solution behaviour for **1** is summarized in Fig. 4.

### 3.2. Biological MTT data

In the MTT assay, **1** was found to have an $IC_{50}$ value of $360 \pm 20$ μM, and **3** had a value of $55 \pm 15$ μM, these being based on averages of two trials; these numbers come from data such as those shown in Fig. 5 that presents graphs of cell viability versus the concentration of the complexes. Both complexes thus show some anticancer activity, but are less active than cisplatin where the MTT assay using the same cell line gave a corresponding $IC_{50}$ value of ~10 μM [35]. Nevertheless, these preliminary data are considered promising as the systems are amenable to several approaches of optimization by fine-tuning.

Complex **1** does dissolve in water to generate $[RuCl(p\text{-cymene})(BESE)]Cl$, the chloride salt of **3**, but only a maximum of half of the Ru in **1** can be converted to the ionic form. The nature of the species present in the phosphate buffer saline solutions is uncertain, but the higher activity of **3** strongly suggests the involvement of a cationic species. Recent studies by Sadler's group have shown that the closely analogous complex $[RuCl(p\text{-cymene})(en)]PF_6$ forms adducts (with displacement of the chloro ligand) by the N7 of guanine in DNA oligonucleotides, and the chloro-cation species and related complexes exhibit $IC_{50}$ values of 6–200 μM for a human ovarian cancer cell line compared with values

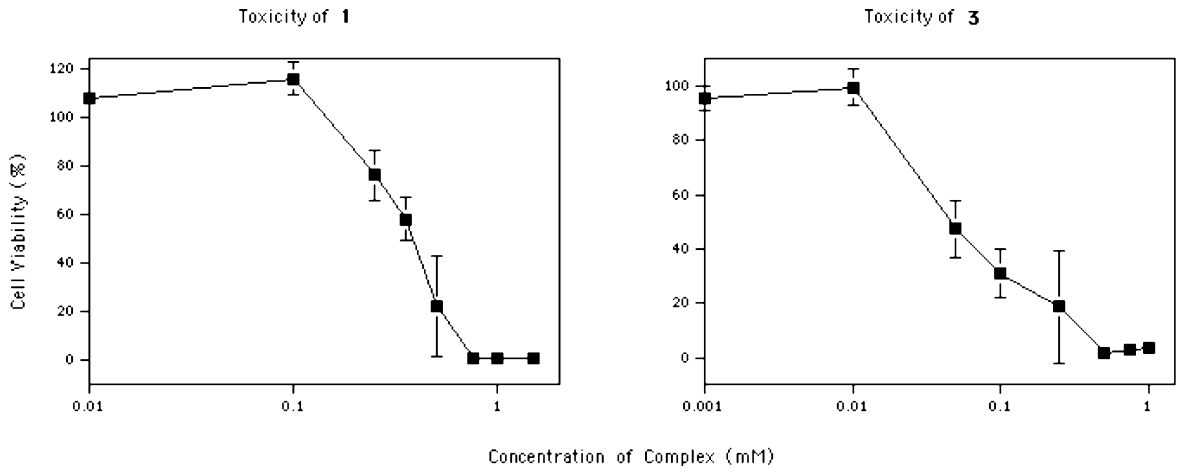


Fig. 5. The MTT assay with $[RuCl_2(p\text{-cymene})]_2(\mu\text{-BESE})$ (**1**) and $[RuCl(p\text{-cymene})(BESE)]PF_6$ (**3**).

of 0.5 μM for cisplatin and 6 μM for carboplatin [18]. The structures of similar, monofunctional guanine adducts of other $[RuCl(\eta^6\text{-arene})(en)]PF_6^-$ complexes have also been determined (where arene = biphenyl, 5,8,9,10-tetrahydroanthracene, and 9,10 dihydroanthracene) [36]. These new findings, coupled with the earlier data on Ru(II)–arene complexes mentioned in Section 1 [13–15], certainly suggest that the mechanism of anticancer activity for Ru(II)–arene complexes involves interaction of cationic derivatives with DNA, with presumably subsequent prevention of DNA replication.

## 4. Supplementary material

Crystallographic data for the structural analysis have been deposited with the Cambridge Crystallographic Data Centre, CCDC Nos. 1-200839 and 200840 for compounds $[RuCl_2(p\text{-cymene})]_2(\mu\text{-BESE})$ (**1**) and $[RuCl(p\text{-cymene})(BESE)]PF_6$ (**3**), respectively. Copies of this information may be obtained free of charge from The Director, CCDC, 12 Union Road, Cambridge, CB2 1EZ, UK (fax: +44-1223-336-033; e-mail: deposit@ccdc.cam.ac.uk or www: http://www.ccdc.cam.ac.uk).

## Acknowledgements

We thank the Natural Sciences and Engineering Research Council of Canada for financial support, and Dr. Kirsten Skov of the Advanced Therapeutics Department at the British Columbia Cancer Research Centre for help with the MTT assays.

## References

[1] (a) Z. Guo, P.J. Sadler, Angew. Chem., Int. Ed. Engl. 38 (1999) 1512;
(b) E. Wang, C.M. Giandomenico, Chem. Rev. 99 (1999) 2451;
(c) E.R. Jamieson, S.J. Lippard, Chem. Rev. 99 (1999) 2467;
(d) J. Reedijk, Chem. Rev. 99 (1999) 2499.
[2] (a) M.J. Clarke, R.D. Galang, V.M. Rodriguez, R. Kumar, S. Pell, D.M. Bryan, in: M. Nicolini (Ed.), Platinum and Other Metal Coordination Compounds in Cancer Chemotherapy, Martinus Nijhoff Publishing, Boston, MA, 1988, p. 582;
(b) M.J. Clarke, F. Zhu, D.R. Frasca, Chem. Rev. 99 (1999) 2511.
[3] R.E. Aird, J. Cummings, A.A. Ritchie, M. Muir, R.E. Morris, H. Chen, P.J. Sadler, D.I. Jodrell, Br. J. Cancer 86 (2001) 1652.
[4] G. Sava, S. Zorzet, T. Giraldi, G. Mestroni, G. Zassinovich, Eur. J. Cancer Clin. Oncol. 20 (1984) 841.
[5] G. Sava, S. Pacor, S. Zorzet, E. Alessio, G. Mestroni, Pharm. Res. 21 (1989) 617.
[6] (a) G. Sava, E. Alessio, A. Bergamo, G. Mestroni, in: M.J. Clarke, P.J. Sadler (Eds.), Metallopharmaceutical I, DNA Interactions, Springer-Verlag, Berlin, 1999, p. 143;
(b) G. Sava, E. Alessio, A. Bergamo, G. Mestroni, Top. Biol. Inorg. Chem. 1 (1999) 143.
[7] E. Alessio, G. Mestroni, G. Nardin, W.M. Attia, M. Calligaris, G. Sava, S. Zorzet, Inorg. Chem. 27 (1988) 4099.
[8] E. Alessio, G. Balducci, A. Lutman, G. Mestroni, M. Calligaris, W.M. Attia, Inorg. Chim. Acta 203 (1993) 205.
[9] P.K.L. Chan, P.K.H. Chan, D.C. Frost, B.R. James, K.A. Skov, Can. J. Chem. 66 (1988) 117.
[10] P.K.L. Chan, B.R. James, D.C. Frost, P.K.H. Chan, H.-L. Hu, K.A. Skov, Can. J. Chem. 67 (1989) 508.
[11] D.T.T. Yapp, S.J. Rettig, B.R. James, K.A. Skov, Inorg. Chem. 36 (1997) 5635.
[12] (a) E.L.S. Cheu, PhD dissertation, University of British Columbia, Vancouver, 2000.;
(b) E.L.S. Cheu, S.J. Rettig, K.A. Skov, B.R. James, 81st Can. Soc. Chem. Conf., Whistler, BC, 1998, Abstract 459.;
(c) E.L.S. Cheu, S.J. Rettig, K.A. Skov, B.R. James, 82nd Can. Soc. Chem. Conf., Toronto, ON, 1999, Abstract 260.
[13] L. Dale, J.H. Tocher, T.M. Dyson, D.I. Edwards, D.A. Tocher, Anti-Cancer Drug Des. 7 (1992) 3.
[14] Y.N. Vashisht Gopal, D. Jayaraju, A.K. Kondapi, Biochem. 38 (1999) 4382.

[15] S. Korn, W. Sheldrick, Inorg. Chim. Acta 254 (1997) 85.
[16] T.J. Mosmann, J. Immun. Methods 65 (1983) 55.
[17] C.S. Allardyce, P.J. Dyson, D.J. Ellis, S.L. Heath, Chem. Commun. (2001) 1396.
[18] (a) R.E. Morris, R.E. Aird, P. del Socorro Murdoch, H. Chen, J. Cummings, N.D. Hughes, S. Parsons, A. Parkin, G. Boyd, D.I. Jodrell, P.J. Sadler, Med. Chem. 44 (2001) 3616;
(b) J. Cummings, R.E. Aird, R.E. Morris, H. Chen, P. del Socorro Murdoch, P.J. Sadler, J.F. Smyth, D.I. Jodrell, Clin. Cancer Res. 6 (2000), Abstract 142.
[19] M. Hull, T.W. Bargar, J. Org. Chem. 40 (1975) 3152.
[20] N. Khiar, C.S. Araújo., F. Alcudia, I. Fernández, J. Ord, Chem. 67 (2002) 345.
[21] C.S. Araujo, L.A. Huxham, N. Khiar, B.R. James, in press.
[22] (a) M.A. Bennett, A.K. Smith, J. Chem. Soc., Dalton Trans. (1974) 233.;
(b) M.A. Bennett, T.-N. Huang, T.W. Matheson, A.K. Smith, Inorg. Syn. 21 (1982) 74.
[23] d*TREK, 4.13 ed., Molecular Structure Corporation, 1996–1998.
[24] W.T. Bellamy, Drugs 44 (1992) 690.
[25] M.C. Alley, D.A. Scudiero, A. Monks, M.L. Hursey, M.J. Czerwinski, D.L. Fine, B.J. Abbott, J.G. Mayo, R.H. Shoemaker, M.R. Boyd, Cancer Res. 48 (1988) 589.
[26] (a) M. Calligaris, O. Carugo, Coord. Chem. Rev. 153 (1996) 83;
(b) M. Calligaris, Croat. Chem. Acta 72 (1999) 147.
[27] G. Orpen, L. Braumer, F.H. Allen, O. Kennard, D.G. Watson, J. Chem. Soc., Dalton Trans. (1989) S1.
[28] J.A. Davies, Adv. Inorg. Chem. Radiochem. 24 (1981) 115.
[29] (a) S. Geremia, M. Calligaris, S. Mestroni, Inorg. Chim. Acta 292 (1999) 144;
(b) M. Calligaris, A. Melchior, S. Geremia, Inorg. Chim. Acta 323 (2001) 89.
[30] C.C. Carvalho, R.H.P. Francisco, M.T.P. Gambardella, G.F. de Souza, C.A.L. Filgueiras, Acta Crystallogr., C 52 (1996) 1627.
[31] R.H.P. Francisco, M.T.P. Gambardella, A.M.D.D. Rodrigues, G.F. de Souza, C.A.L. Filgueiras, Acta Crystallogr., C 51 (1995) 604.
[32] (a) T. Tanase, T. Aiko, Y. Yamamoto, Chem. Commun. (1996) 2341.;
(b) S. Geremia, G. Mestroni, M. Calligaris, E. Alessio, J. Chem. Soc., Dalton Trans. (1998) 2447.
[33] W.J. Geary, Coord. Chem. Rev. 7 (1971) 110.
[34] R.A. Zelonka, M.C. Baird, Can. J. Chem. 50 (1972) 3063.
[35] J. Sartor, L. Mayer, Personal communication (BC Cancer Research Centre), 2001.
[36] C. Haimei, J.A. Parkinson, S. Parsons, R.A. Coxall, R.O. Gould, P.J. Sadler, J. Am. Chem. Soc. 124 (2002) 3064.